Mutual Impedance Computation Between Printed Dipoles

NICOLAOS G. ALEXOPOULOS, MEMBER, IEEE, AND INAM E. RANA

Abstract—**The mutual impedance between microstrip dipoles printed on a grounded substrate is computed. Results for the microstrip dipoles in broadside, collinear, and echelon arrangements are presented. The significance of surface waves to mutual coupling is discussed.**

I. INTRODUCTION

MICROSTRIP dipoles have been previously used in a conformal configuration [1]. Unfortunately, there are no design criteria for such elements due to the analytical complexity introduced by the presence of the grounded dielectric substrate. Extensive mutual impedance data exist for an assumed current distribution when the relative dielectric constant of the substrate is unity [2].

In this paper the mutual coupling properties of microstrip dipoles will be investigated in broadside, collinear, and echelon arrangements. The computation of mutual impedance for printed dipoles is a complex problem since in addition to the space wave, surface waves become significant contributors to mutual interaction among the array elements. The element interaction due to surface wave modes remains significant even for a relatively large separation between microstrip dipoles. This is due to the fact that the dielectric substrate is a wave-guiding structure for transverse electric (TE) and transverse magnetic (TM) modes, with the basic TM mode having no cut-off [3], [4]. The substrate thickness and relative dielectric constant determine the number of surface wave modes which the substrate can support for a given frequency. This in fact has been found to have a fundamental influence on the printed antenna current distribution [5].

In the computation of mutual coupling, it is inadequate in this case to assume a current distribution, due mainly to the presence of surface wave modes. Since the surface modes influence the current distribution even for array elements many wavelengths apart, it is of paramount importance that the precise current distribution is determined. This necessitates the correct formulation of the integral equation for the unknown currents over two printed dipoles, as e.g., shown in Fig. 1, where the two printed dipoles are shown for generality in an echelon configuration. The formulation of the integral equation involves the Green's function which satisfies all the boundary conditions to the problem. The Green's function is in terms of the Sommerfeld type of integrals [6], [7], whose derivatives are improper integrals when the field and source points are on the substrate. A method which resolves this difficulty has been derived [4], [5], and the antenna current distribution over the two antennas can be obtained.

Manuscript received November 30, 1979; revised July 23, 1980. This work was supported by the U.S. Army under Contract DAAG29-79-C-0050.

N. G. Alexopoulos is with the Department of Electrical Science and Engineering, University of California, Los Angeles, CA 90024.

I. E. Rana is with Suparco, P.O. Box 3209, Karachi 28, Pakistan.

II. FORMULATION OF THE MUTUAL IMPEDANCE PROBLEM

In order to compute the current distribution over the microstrip dipoles shown in Fig. 1, the radius of the dipoles is assumed to be much smaller than that of the free space wavelength $a = 0.00001\ \lambda_0$. The current distribution over a pair of dipoles in a broadside configuration can be expressed, for example, by

$$J(x', y') = [I_1(x')\delta(y')P_1 + I_2(x')\delta(y' - S)P_2]\,\delta(z' - B)\hat{x} \tag{1}$$

where $I_1(x')$, $I_2(x')$ are the unknown currents and P_1, P_2 are two unit pulse functions which are zero everywhere except over the lengths of the dipoles L_1, L_2, respectively. The axial component of the electric field E_x is given at any point on the substrate by [5], [8],

$$E_x = \int_{L_1, y'=0} I_1(x')\left[k^2\Pi_x + \frac{\partial^2\Pi_x}{\partial x^2} + \frac{\partial^2\Pi_z}{\partial x \partial z}\right]dx' + \int_{L_2, y'=S} I_2(x')\left[k^2\Pi_x + \frac{\partial^2\Pi_x}{\partial x^2} + \frac{\partial^2\Pi_z}{\partial x \partial z}\right]dx' \tag{2}$$

where the components of the Hertz vector Π_x, Π_z are given by [5]

$$\Pi_x = \lim_{z \to B} 2K \int_0^\infty J_0(\lambda\rho)e^{-\mu(z-B)}\frac{\lambda\, d\lambda}{D_e(\lambda)} \tag{3}$$

and

$$\Pi_z = \lim_{z \to B} 2K(1 - \epsilon_r) \int_0^\infty J_1(\lambda\rho)e^{-\mu(z-B)}\frac{\lambda^2 \cos\phi\, d\lambda}{D_e(\lambda)D_m(\lambda)} \tag{4}$$

with

$$D_e(\lambda) = \mu + \mu_e \coth \mu_e B, \tag{5}$$

$$D_m(\lambda) = \mu\epsilon_r + \mu_e \tanh \mu_e B, \tag{6}$$

$$\mu = [\lambda^2 - k^2]^{1/2},\ \mu_e = [\lambda^2 - \epsilon_r k^2]^{1/2},\ K = -\frac{j}{4\pi\epsilon_0\omega}$$

and

$$\rho = [(x - x')^2 + (y - y')^2]^{1/2}.$$

In order to solve for $I_1(x')$, $I_2(x')$ each of the dipoles is divided into N_1, N_2 subsections, respectively. Galerkin's

0018-926X/81/0100-0106$00.75

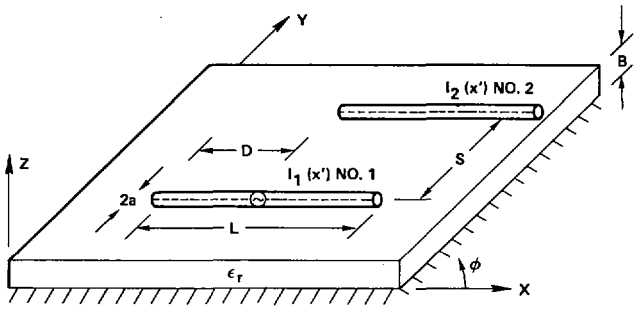

Fig. 1. Mutual coupling geometry.

method is then adopted with sinusoidal expansion and testing functions. With this choice of expansion and testing functions and with the appropriate principal value integration of the Sommerfeld-type integrals along the real axis [5], [7], $I_1(x')$ and $I_2(x')$ can be obtained by inversion of the system of equations,

$$\begin{bmatrix} V_1 \\ V_2 \\ \cdot \\ \cdot \\ V_M \end{bmatrix} = \begin{bmatrix} Z_{11}, Z_{12}, \cdots Z_{1M} \\ Z_{21}, Z_{22}, \cdots Z_{2M} \\ \cdot \quad \cdot \quad \cdot \\ \cdot \quad \cdot \quad \cdot \\ Z_M, \qquad Z_{MM} \end{bmatrix} \begin{bmatrix} I_1 \\ I_2 \\ \cdot \\ \cdot \\ I_M \end{bmatrix} \tag{7}$$

where $M = N_1 + N_2 - 2$.

Depending upon the location of the generator, the corresponding excitation voltage is set to one. The inversion of the matrix then gives the current distribution on the dipole parasitic pair. This method can further be extended to any number of printed dipoles, parasitic or active. Knowledge of the current distribution over the pair is used to determine the mutual impedance between the printed dipoles. The input impedance of the two dipole printed array is given by

$$Z_{\text{in}} = Z_{11} + Z_{12} \cdot I_2/I_1 \tag{8}$$

where Z_{11} is the self impedance of the driven dipole when the parasitic dipole is open circuited. Also, Z_{12} is the mutual impedance between the pair, whereas I_1 and I_2 are the input currents which flow into the input terminal of the driven dipole and across the short-circuited input terminals of the parasitic dipole. For unit voltage excitation, i.e., $V = 1.0$ volts, the input impedance of the array is given by

$$Z_{\text{in}} = 1.0/I_1. \tag{9}$$

The self impedance Z_{11} of the driven dipole is obtained numerically by deleting the $(N_1 + N_2/2 - 1)$th row and column of the matrix equation (7) and inverting the resultant $(N_1 + N_2 - 3)$th order matrix. Physically this operation means open circuiting the parasitic dipole. The input current of the driven dipole I_1' gives the self impedance Z_{11} as

$$Z_{11} = 1.0/I_1'. \tag{10}$$

When (9) and (10) are inserted in (8), the mutual impedance between the two printed dipoles is given by

$$Z_{12} = 1.0/I_2 - I_1/(I_1' \cdot I_2). \tag{11}$$

III. FIELDS EXCITED BY A PRINTED DIPOLE ALONG AIR DIELECTRIC INTERFACE

Mutual coupling between two printed dipoles is dominantly determined by the fields which exist along the air dielectric interface. The fields excited by a printed dipole along the air dielectric interface can be decomposed into the following components [3]: a space wave ($1/\rho$ dependence), a higher order wave ($1/\rho^2$ dependence), a surface wave ($1/\rho^{1/2}$ dependence) and leaky waves ($\exp(-\lambda\rho)/\rho^{1/2}$ dependence), $\lambda > 0$. This decomposition can be explained in the context of the saddle point integration method. The saddle point and its vicinity contribute to the direct wave, while for small ρ, the integration over the rest of the steepest descent path (SDP) is significant, and results in higher order waves. The surface and leaky waves are contributed by the poles which the integration contour crosses during its deformation to the SDP.

As ρ increases the surface waves constitute the dominant contribution because of their cylindrical wave character $1/\rho^{1/2}$ as opposed to the spherical behavior of the space wave.

The number of surface wave modes generated by the antenna depends upon the thickness and dielectric constant of the substrate. The lowest order mode is the TM mode with a component of electric field parallel to the direction of propagation [4]. Assuming a single propagating mode, the antenna will generate a longitudinal component of the electric field which will be strongest near the tips of the dipole. A strong surface wave will therefore be launched along the axis of the printed antenna. In the broadside direction ($\phi = 90°$), a component of the electric field exists which is transverse to the direction of propagation. Therefore, the TM mode of the surface wave will not be excited. On the other hand, if the dielectric substrate guide allows two propagating surface wave modes, then in the broadside direction the TE mode of the surface is excited.

Mathematically this spatial dependence can be viewed as follows. The lowest order TM mode is contributed by the denominator $D_m(\lambda)$ of the component Π_z of the Hertz vector $\bar{\Pi}$. Expression [4] for Π_z contains a factor $\cos\phi$ which determines the spatial variation of the surface wave.

From the above discussion, one concludes that for a single propagating mode, the mutual coupling in broadside arrangement is mainly due to the direct, higher order, and leaky waves, while in the collinear arrangement, dominant coupling is due to the TM mode of the surface waves. However, for two propagating modes, dominant coupling in the broadside configuration is due to the TE mode of the surface waves, while in the collinear configuration, it is due to the TM mode.

IV. NUMERICAL RESULTS

Mutual impedance computations between two printed dipoles have been performed in three configurations: 1) broadside, 2) collinear, and 3) echelon.

As it was discussed previously, the lowest order surface wave mode, i.e., TM, has a launching pattern $\cos\phi$. This means that when two dipoles are in a broadside configuration ($\phi = 90°$), the part of the total coupling due to the surface wave will be minimum. The coupling in this configuration will be mainly due to direct, higher order, and leaky waves excited by the antenna. Fig. 2 and 3 show broadside coupling between the two printed dipoles as a function of separation S for different

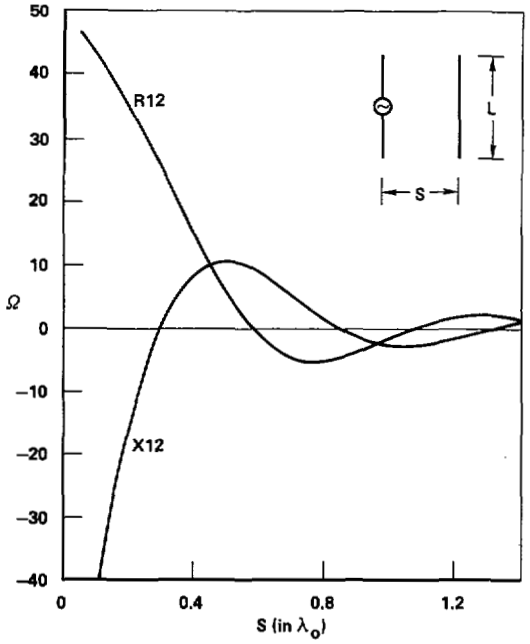

Fig. 2. Mutual impedance between two broadside dipoles versus (B = 0.1016 λ_0, ϵ_r = 3.25, L = 0.333 λ_0).

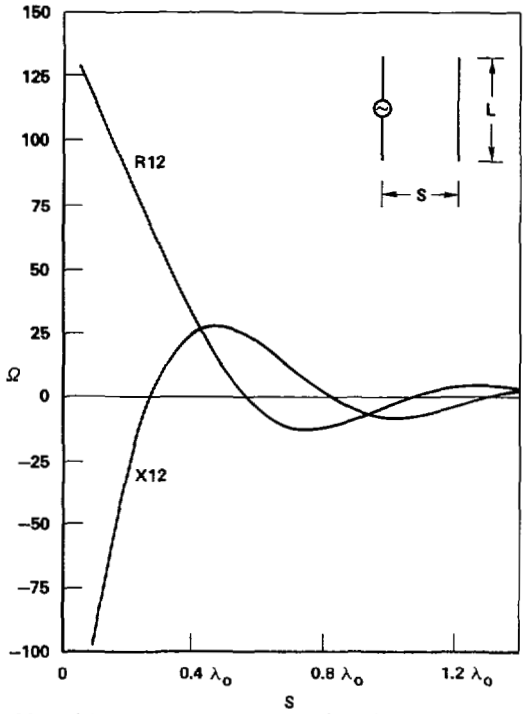

Fig. 3. Mutual impedance between two broadside dipoles versus (B = 0.1016 λ_0, ϵ_r = 3.25, L = 0.4167 λ_0).

antenna lengths. The rapid fall in mutual coupling for small separation ($S < 0.4\ \lambda_0$) confirms that the coupling is mainly due to higher order modes, while for ($S > 0.8\ \lambda_0$) the space (direct) wave takes over. In the intermediate zone ($0.4\ \lambda_0 < S < 0.8\ \lambda_0$), leaky wave modes are dominant.

The printed dipole launches a surface wave with maximum efficiency along the axial direction ($\phi = 0^\circ$). Also, the radiation pattern of a dipole in free space has nulls along the axial directions ($\phi = 0^\circ$ and $\phi = 180^\circ$). Therefore, based on these arguments, it can be concluded that in the collinear arrangement, the mutual coupling will be mainly due to the surface wave. The surface waves decay as $1/\rho^{1/2}$. Hence mutual coupling should decay slowly in this configuration. Figs. 4–6 show mutual impedance for the collinear case plotted versus separation G, for different dipole lengths. Mutual coupling decays very slowly with G. The period of oscillation of the mutual impedance as obtained from Fig. 4 is 0.88 λ_0, while the wavelength of the excited surface wave is 0.8811 λ_0. This agreement is excellent and confirms that mutual coupling for the collinear configuration is only due to the TM mode of the surface waves. The initial behavior for small G is due to the near zone field of the dipoles, as is clear from Fig. 7.

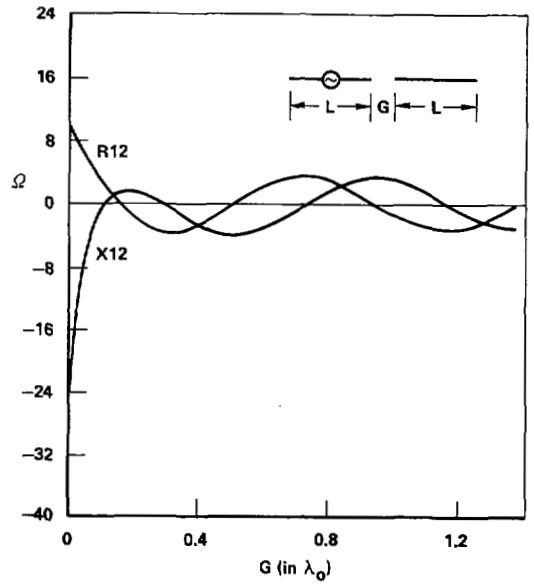

Fig. 4. Mutual impedance between two collinear dipoles versus (B = 0.1016 λ_0, ϵ_r = 3.25, L = 0.25 λ_0).

In the echelon configuration, mutual impedance computations versus displacement D are shown in Fig. 8 and 9 for different dipole lengths. For $D = 0\ \lambda_0$, the dipoles are in the broadside configuration, while for D large, the dipoles are approximately collinear. As D increases, Z_{12} decreases rapidly from the broadside value and ultimately shows the same behavior, as shown by the dipoles in collinearity.

The efficiency of the surface wave excitation depends upon the thickness of the substrate B for a given dielectric constant ϵ_r. To observe this effect, the substrate thickness is next increased from 0.1016 λ_0 to 0.127 λ_0, and computations for mutual impedance between the dipoles in collinear arrangement are performed. A result is shown in Figs. 10 and 11. These results are compared with the ones shown in Figs. 5 and 6. The comparison indicates that the surface wave launching efficiency increases with the thickness of the substrate.

Next two propagating surface wave modes are allowed by increasing the substrate thickness to 0.15 λ_0 and the dielectric constant to 8.5. Computations for dipoles in broadside and collinear configuration are performed. After investigation of the effect of different dipole lengths (see, e.g., Figs. 11 and 12) the following comments are in order.

1) The period of oscillation of the mutual impedance between two collinear dipoles as obtained form the graph is 0.42 λ_0, while the wavelength of the TM mode from the computer program is 0.408 λ_0. This agreement is good and proves that the coupling in collinear arrangement is dominantly due to the TM mode of the surface waves.

2) Mutual coupling is small for this collinear agreement. This is due to the fact that most of the surface wave power carried by this mode flows inside the dielectric substrate.

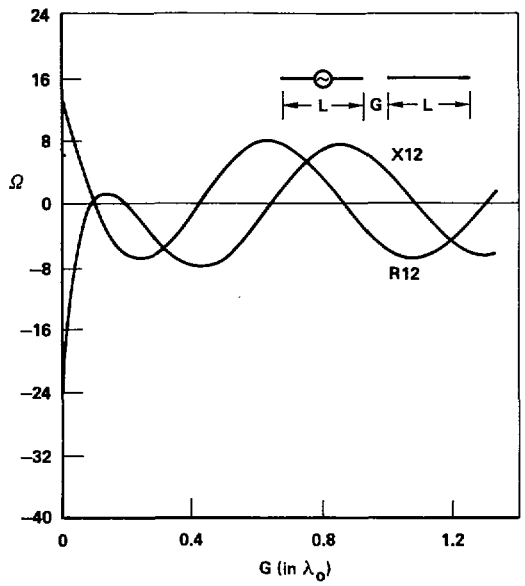

Fig. 5. Mutual impedance between two collinear dipoles versus (B = 0.1016 λ_0, ϵ_r = 3.25, L = 0.33 λ_0).

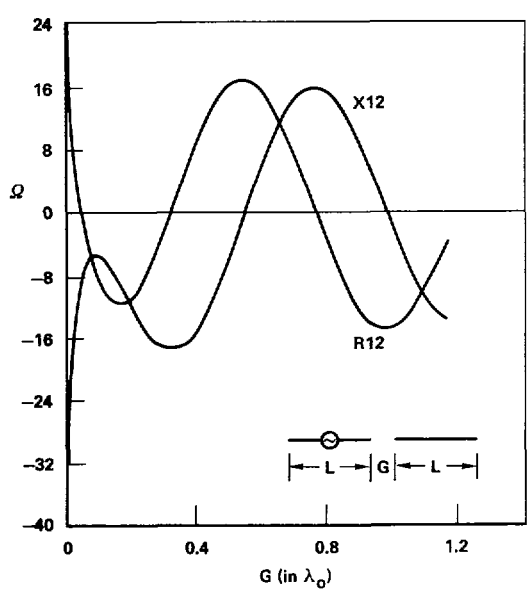

Fig. 6. Mutual impedance between two collinear dipoles versus (B = 0.1016 λ_0, ϵ_r = 3.25, L = 0.4167 λ_0).

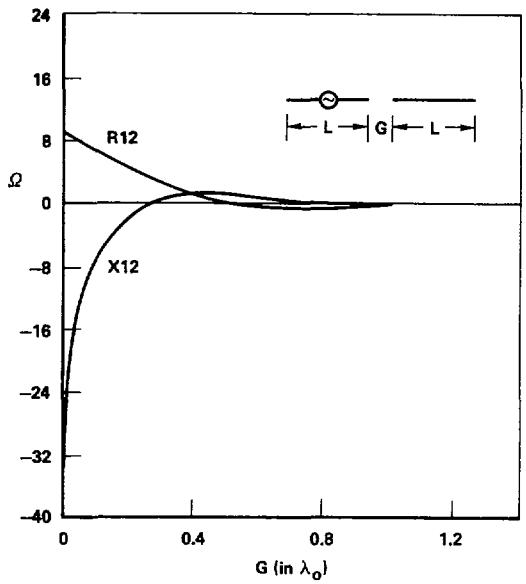

Fig. 7. Mutual impedance between two collinear dipoles versus (B = 0.1016 λ_0, ϵ_r = 1.0, L = 0.4167 λ_0).

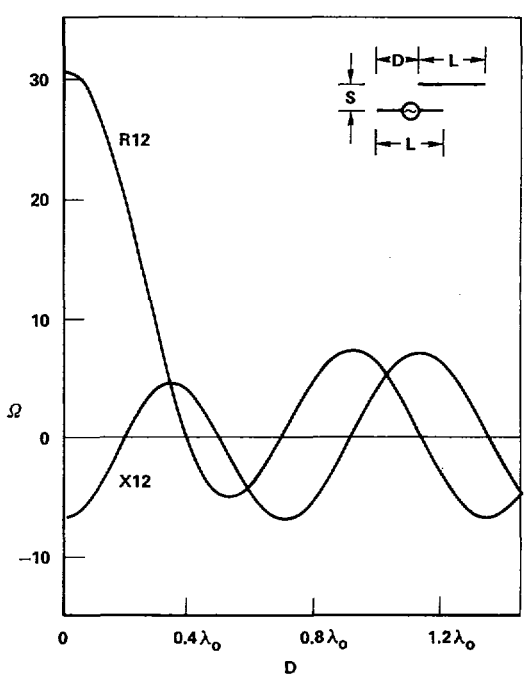

Fig. 8. Mutual impedance between two dipoles in echelon versus (B = 0.1016 λ_0, ϵ_r = 3.25, L = 0.333 λ_0, S = 0.25 λ_0).

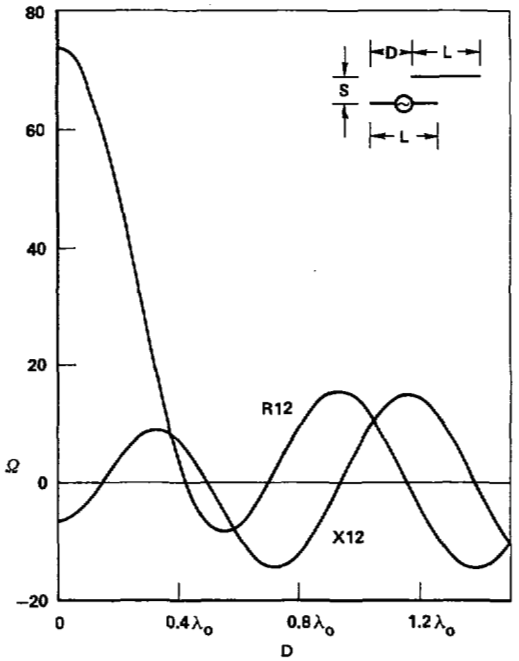

Fig. 9. Mutual impedance between two dipoles in echelon versus (B = 0.1016 λ_0, ϵ_r = 3.25, L = 0.4167 λ_0, S = 0.25 λ_0).

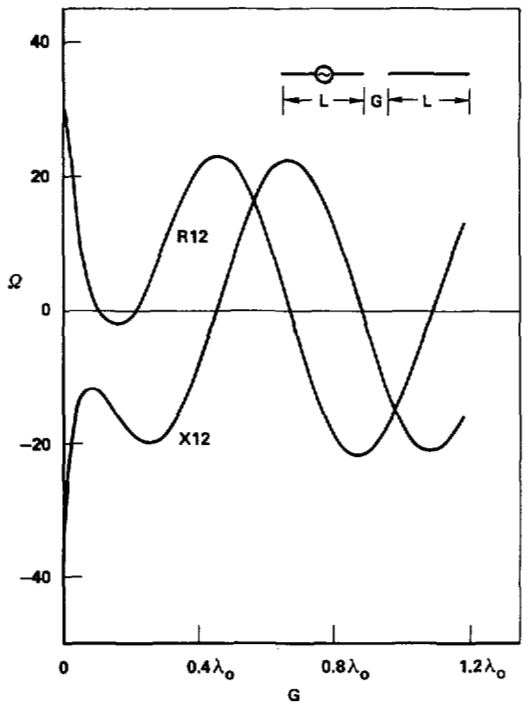

Fig. 11. Mutual impedance between two collinear dipoles versus (B = 0.127 λ_0, ϵ_r = 3.25, L = 0.4 λ_0).

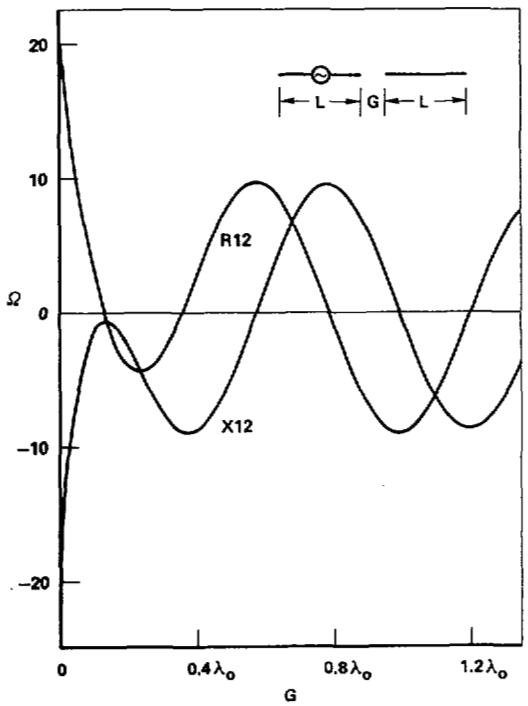

Fig. 10. Mutual impedance between two collinear dipoles versus (B = 0.1016 λ_0, ϵ_r = 3.25, L = 0.3 λ_0).

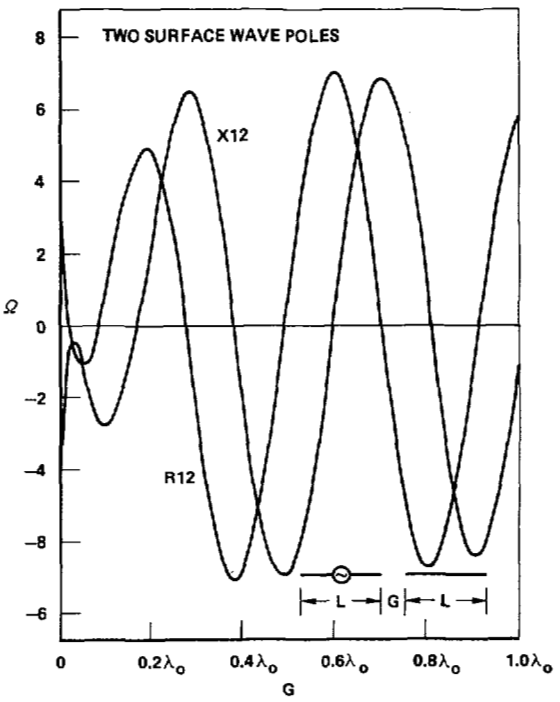

Fig. 12. Mutual impedance between two collinear dipoles versus (B = 0.1016 λ_0, ϵ_r = 8.5, L = 0.25 λ_0).

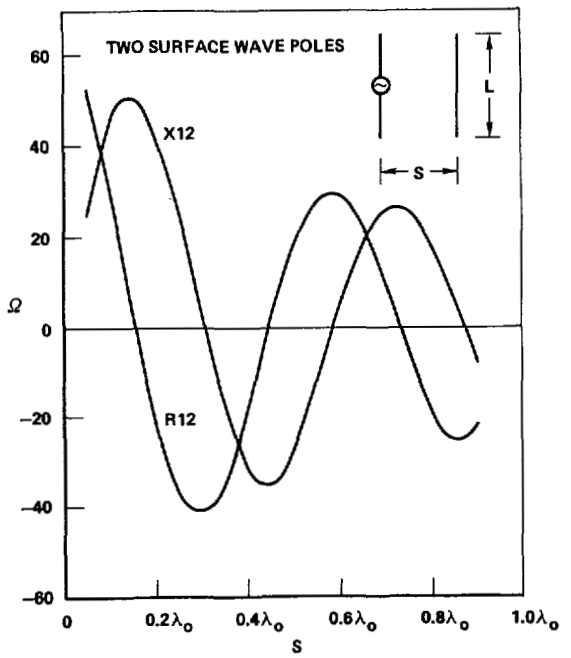

Fig. 13. Mutual impedance between two broadside dipoles versus (B = 0.15 λ_0, L = 0.3 λ_0, ϵ_r = 8.5).

For the broadside situation (see, e.g., Figs. 12 and 13) the following points are noted.

1) The mutual impedance plot oscillates with a period of 0.566 λ_0 which is close to the wavelength of the TE mode of the surface waves, i.e., 0.533 λ_0. This proves that mutual impedance in the broadside configuration is mainly due to the TE mode of the surface wave.

2) The decay in coupling is rather rapid as compared to the collinear case.

V. CONCLUSION

In this paper the mutual impedance between microstrip dipoles in broadside, collinear, and echelon configurations has been computed. It has been determined that surface waves enhance mutual coupling in a collinear arrangement of the printed dipoles. In addition it has been concluded that surface waves decay in a manner inversely proportional to the square root of element separation and that therefore their contribution to mutual coupling may be significant, even when the array elements are several wavelengths apart.

ACKNOWLEDGMENT

The authors wish to thank Professor R. S. Elliott for helpful discussions and Ms. C. Kaplan and Ms. P. Stebbins for typing the manuscript.

REFERENCES

[1] J. C. Williams, "Cross fed printed antennas," in *8th European Microwave Conf. Proc.*, Copenhagen, 1977, pp. 292–296.

[2] H. C. Baker and A. H. LaGrone, "Digital computation of the mutual impedance between thin dipoles," *IRE Trans. Antennas Propagat.*, pp. 172–178, Mar. 1962.

[3] L. B. Felsen and N. Marcuvitz, *Radiation and Scattering of Waves, Microwaves, Fields Series*. Englewood Cliffs, NJ: Prentice-Hall, 1973.

[4] N. K. Uzunoglu, N. G. Alexopoulos, and J. G. Fikioris, "Radiation properties of microstrip dipoles," *IEEE Trans. Antennas Propagat.*, vol. AP-27, pp. 853–858, Nov. 1979.

[5] I. E. Rana and N. G. Alexopoulos, "Current distribution and input impedance of printed dipoles," *IEEE Trans. Antennas Propagat.*, vol. AP-29, pp. 99–105, Jan. 1981, this issue.

[6] A. Sommerfeld, *Partial Differential Equations in Physics*. New York: Academic, 1949, vol. VI.

[7] J. A. Stratton, *Electromagnetic Theory*. New York: McGraw-Hill, 1941.

[8] I. E. Rana, "On the theory and design of printed antenna arrays," Ph.D. dissertation, Univer. of California, Los Angeles, 1979.

Nicolaos G. Alexopoulos (S'68–M'69), for biography and photograph please see page 105 of this issue.

Inam E. Rana, for biography and photograph please see page 105 of this issue.